ARTICLE

Layered Metal Phosphonate Reinforced Poly(L-lactide) Composites with a Highly Enhanced Crystallization Rate

Pengju Pan,[†] Zhichao Liang,[†] Amin Cao,[‡] and Yoshio Inoue*[,†]

Department of Biomolecular Engineering, Tokyo Institute of Technology, 4259-B-55 Nagatsuta, Midori-ku, Yokohama 226-8501, Japan, and Laboratory for Polymer Materials, Shanghai Institute of Organic Chemistry, Chinese Academy of Sciences, Shanghai 200032, China

ABSTRACT Layered metal phosphonate, zinc phenylphosphonate (PPZn), reinforced poly(L-lactide) (PLLA) composites were fabricated by a melt-mixing technique. The nonisothermal and isothermal crystallization, melting behavior, spherulite morphology, crystalline structure, and static and dynamic mechanical properties of the PLLA/PPZn composites were investigated. PPZn shows excellent nucleating effects on PLLA crystallization. With incorporation of 0.02% PPZn, PLLA can finish crystallization under cooling at 10 °C/min. The crystallization rate of PLLA further increases with increasing PPZn concentration. Upon the addition of 15% PPZn, the crystallization half-times of a PLLA/PPZn composite decrease from 28.0 to 0.33 min at 130 °C, and from 60.2 to 1.4 min at 140 °C, compared to the neat PLLA. With the presence of PPZn, the nuclei number of PLLA increases and the spherulite size reduces significantly. Through analysis of the crystal structures of PLLA and PPZn, it was proposed that the nucleation mechanism of the PLLA/PPZn system is epitaxial nucleation. The incorporation of PPZn has no discernible effect on the crystalline structure of PLLA. Moreover, PPZn has good reinforcement effects on the PLLA matrix. The tensile strength of the composite is enhanced with the addition of a relatively small amount of PPZn (<5%). The tensile and storage moduli of composites increase with increasing PPZn loadings, and they respectively improve by 28% and 34% with the incorporation of a 15% PPZn filler, as compared to the neat PLLA.

KEYWORDS: poly(L-lactide) • zinc phenylphosphonate • crystallization • nucleating agent • mechanical properties

INTRODUCTION

Poly(L-lactide) (PLLA) bioplastic has been attracting considerable attention from both fundamental and practical perspectives because it is biomass-derived, biodegradable, biocompatible, and nontoxic to the environment and human body (1). Because its degradation products are bioresorbable, this polymer is one of the select few candidates for use in biomedical applications such as surgical sutures, bone fixation devices, and controlled drug-delivery systems. Besides, because of its favorable biodegradability, good mechanical properties, and versatile fabrication processes, it has excellent potential for substitution of petroleum-based polymers (2). However, there is a critical issue concerning the crystallization rate of PLLA. Despite the fact that PLLA is a semicrystalline polymer, almost no crystallization proceeds under fast cooling such as a practical molding condition (3). This poor processability is one of the major drawbacks of PLLA-based materials.

In general, the crystallization process of polymers is divided into two main stages, that is, nucleation and crystal growth. A primary nucleation process may be either homogeneous or heterogeneous. Homogeneous nucleation stems from the statistical fluctuations of polymer chains in the melt and is characterized by a constant rate. However, the heterogeneous one occurs at relatively low supercooling because of the presence of foreign bodies in the polymer melt that increase the crystallization rate, acting as heterogeneous nuclei and reducing the free energy needed for the formation of a critical nucleus. These additives, which have high performance in the acceleration of nucleation, are called "nucleating agents (NAs)" (4). NAs induce the higher crystallization temperatures and degree of crystallinity and thus can improve the processability, productivity in mold processing, and thermal, mechanical, and optical properties of semicrystalline polymers (4). From the economical and cost-effective viewpoints, the suitable utilization of NAs is one of the solutions to the issues in the practical application of polymeric materials.

Up to now, many kinds of NAs have been successfully developed and their effects on the crystallization behavior have been studied for many semicrystalline polymers including isotactic polypropylene (iPP) (4−9), poly(ethylene terephthalate) (PET) (10), poly(vinylidene fluoride) (11), and some biodegradable polymers like poly(3-hydroxybutyrate) (12−14), poly(butylene adipate) (PBA) (15), and poly(butylene succinate) (PBS) (16), and so on. A few NAs of PLLA have also been reported by several research groups (3, 17−21). Several authors (17−19) have found that the crystallization rate of PLLA increases with the addition of poly(D-lactide)

* To whom corresponding should be addressed. Tel.: +81-45-924-5794. Fax: +81-45-924-5827. E-mail: inoue.y.af@m.titech.ac.jp.

Received for review October 8, 2008 and accepted December 10, 2008

[†] Tokyo Institute of Technology.

[‡] Chinese Academy of Sciences.

DOI: 10.1021/am800106f

Published on Web 01/07/2009

(PDLA) because of the nucleation effect of PLLA/PDLA stereocomplex crystallites. Okamoto et al. (20) have used a low-molecular-weight aliphatic amide as NA for PLLA and studied the crystallization kinetics and morphology of this PLLA/NA system. Kawamoto et al. (3) have found that some hydrazide compounds can accelerate the crystallization of PLLA and investigated the relationship between the chemical structure and nucleation efficiency of these kinds of NAs.

Although PLLA possesses relatively good thermal and mechanical properties among the family of biodegradable polymers, its mechanical strength, modulus, and heat-resistance properties are not good enough for some applications. Recently, there have been several attempts to modify the end-use properties of PLLA by fabricating the composites with inorganic fillers such as layered silicate (22−28). With the incorporation of layered silicate, the mechanical, heat-resistance, and gas-barrier properties of PLLA can be improved (22−26). Moreover, the biodegradability of these PLLA biocomposites also depends on the nature of the layered silicate, making it possible to tailor the material's biodegradability by adding an appropriate organically modified clay (27). However, the layered silicate fillers usually have very limited nucleating effects on the crystallization of PLLA, and thus NAs are required when processing and molding these polymeric composites.

Metal phosphonate is a kind of synthetic inorganic/organic hybrid material with a layered structure that is similar to montmorillonite clay. To date, several attempts have been made to fabricate the metal phosphonate reinforced polymeric composites (29−32). With the incorporation of layered metal phosphonates (e.g., α-zirconium phosphate), the mechanical properties and thermal stability of polymers such as epoxy (29, 30), poly(acrylamide) (31), and PET (32) can be modified. The applications of metal phosphonates have been extended to the fields including catalysts (33), chemical sensors (34), sorbents (35), ferromagnets (36), and ion exchangers (37). Besides, metal phosphonates can find applications in the field of biomaterials because phosphate is a naturally occurring functional group. For example, calcium phosphate appears to be a good candidate as implants for bone reconstruction (38). Bujoli et al. (39) suggested that the metal phosphonates are potential materials for developing oligonucleotide microarrays, protein binding, and drug-delivery systems. Herschke et al. (40) reported that zinc phosphate is a versatile material for potential biomedical applications such as bone replacement cements. Moreover, the properties of metal phosphonates can be manipulated in a wide range by changing the types of metal ions or organic groups. On the other hand, very recently, Mitomo et al. (21) reported that the metal phosphonate materials can accelerate the crystallization of PLLA, although the detailed crystallization kinetics and nucleation mechanism of these PLLA/NA systems are still unclear. Therefore, it is considered that the layered metal phosphonate materials might be a kind of promising filler because of its potential ability to improve both the mechanical properties and crystallization rate of PLLA.

Very recently, a new crystal modification, named the α′ form (disordered α), has been proposed for PLLA crystallized at low temperatures (<100 °C), different from the ordered α form crystallized at high temperatures (>120 °C) (41−44). As we know, a broad range of properties of polymorphic polymers, for instance, thermal and mechanical properties and biodegradability (of biodegradable polymers) (45−48), are dependent on the crystalline structure as well as morphology. Besides, it has been reported that the crystal polymorphs of semicrystalline polymers can be regulated by the use of NAs (4, 9, 11, 15). Despite many studies on the crystallization behavior of PLLA-based composites and PLLA/NA systems, to our knowledge, the effects of fillers or NAs on the formation of PLLA α and α′ crystals have hardly been studied.

In this work, we selected zinc phenylphosphonate (PPZn) as a model metal phosphonate material and fabricated the PLLA/PPZn composites with different filler contents by the melt-mixing technique. The nonisothermal and isothermal crystallization kinetics, spherulite morphology, and crystalline structure of the composites were systematically investigated. The static and dynamic mechanical properties of PLLA/PPZn composites were examined. Moreover, the nucleation mechanism of the PLLA/PPZn system was discussed.

EXPERIMENTAL SECTION

Materials. PLLA (M_n = 121 kg/mol; M_w/M_n = 1.54) was kindly supplied by Shimadzu Co. (Kyoto, Japan). PDLA (M_n = 210 kg/mol; M_w/M_n = 1.33) was prepared via the ring-opening polymerization of D-lactide. $ZnCl_2$, phenylphosphonic acid, and NaOH, which were all analytical grade, were purchased from Kanto Chemical Co., Inc. (Tokyo, Japan). Talc (in the powder form) was purchased from Toyo Kasei Kogyo Co. Ltd. (Tokyo, Japan). All of these chemicals were used as received.

Synthesis of PPZn. Zinc phenylphosphonate monohydrate was prepared according to the published procedure (49). Typically, 1 g of phenylphosphonic acid was dissolved in 40 mL of water. A total of 1 equiv of $ZnCl_2$ dissolved in 20 mL of water was added to the stirred phenylphosphonic acid solution, followed by the addition of drops of 0.1 M aqueous NaOH to reach pH 5−6. The sample was filtered and then stirred in water at 50 °C for 3 days to improve the crystallinity. The sample prepared in this way was filtered, washed with water, and dried at 40 °C under vacuum for 3 days. Finally, this compound was dehydrated by keeping it under vacuum at 200 °C overnight.

Preparation of Composite and Blend Samples. Before mixing, PPZn was milled in a MM200 mixer mill for 5 min at a frequency of 20 Hz. After drying at 40 °C under vacuum for 2 days, PLLA and PPZn (or talc) powder were mixed at 190 °C in a single-screw extruder at a speed of 80 rpm for 3 min. To attain the film sample (with a thickness of 0.35−0.40 mm) for characterization, the PLLA/PPZn samples were hot-pressed at 190 °C after melting for 2 min, followed by a quenching to ∼23 °C between two iron plates under room conditions. The composite and blend samples are denoted as PLLA/*x* % filler (or NA), where *x* % is the weight percent of filler or NA. According to the optical microscopy analysis, the sizes of PPZn in the polymeric matrix are less than 5−10 μm, indicating the nearly homogeneous dispersion of PPZn.

PLLA and 1 wt % PDLA were dissolved in chloroform (∼1 g/50 mL). The solution was cast on a Petri dish, and the solvent was allowed to evaporate at room temperature. Then the blend sample was placed in an oven at 40 °C under vacuum for 48 h to eliminate residual solvent. Pure PLLA and a PLLA/1 % PDLA

blend were also melt-processed under the same conditions to maintain the identical thermal history.

Characterizations. ***Gel Permeation Chromatography (GPC).*** Molecular weight was measured on a Tosoh HLC-8220 GPC system assembled with a Viscotek T-60AV viscometer. Chloroform was used as the eluent at a flow rate of 1.0 mL/min. The polystyrene samples with narrow molecular weight distribution were used as standards to calibrate the GPC elution curve. After melt processing, the molecular weights of neat PLLA and PLLA in composites were investigated. The M_n values of melt-processed neat PLLA and 1%, 2%, 5%, and 10% PLLA/PPZn composites are 107, 104, 99, 102, and 98 kg/mol with M_w/M_n values of 1.64, 1.78, 1.68, 1.74, and 1.79, respectively. The molecular weight of PLLA slightly decreased with thermal processing at high temperature (e.g., at 190 °C for 3 min). The melt-processed neat PLLA and its composites show similar molecular weights, indicating that PPZn little affects the thermal degradation of PLLA in the preparation process used.

Differential Scanning Calorimetry (DSC). The crystallization behavior was measured by a Pyris Diamond DSC instrument (Perkin-Elmer Japan Co.) equipped with an intracooler 2P cooling accessory. The temperature and heat flow at different heating rates were calibrated using an indium standard. The sample (~7 mg) was weighed and sealed in an aluminum pan. To investigate the cold-crystallization behavior, the samples were quenched into liquid nitrogen after melting at 190 °C for 2 min and then heated to 190 °C at 10 °C/min. In the melt crystallization, the samples were cooled from the melt state to 0 °C at 10 °C/min for nonisothermal crystallization or rapidly cooled (at 100 °C/min) to the desired temperature for isothermal crystallization, followed by a reheating to 190 °C at 10 °C/min to observe the melting behavior.

Polarized Optical Microscopy (POM). POM observation was performed on a BX90 polarized optical microscope (Olympus Co., Tokyo, Japan) equipped with a digital camera. The film sample was sandwiched by two glass slides. After melting at 190 °C for 2 min, it was quickly transferred to a hot stage (Mettler FP82HT) preset to 140 or 150 °C for crystallization. The spherulite morphology was recorded after completion of crystallization.

Wide-Angle X-ray Diffraction (WAXD). WAXD patterns were recorded on a Rigaku RU-200 (Rigaku Co., Tokyo, Japan) with Ni-filtered Cu Kα radiation ($\lambda = 0.1542$ nm), working at 40 kV and 200 mA. WAXD patterns of PPZn, quenched, and melt-crystallized composite samples were recorded in the 2θ ranges of 1−50° or 5−50° with a scan rate of 1°/min.

Fourier Transform Infrared (FTIR) Spectroscopy. FTIR spectra of the crystallized samples were measured using an FTIR microscope (AIM-8800; Shimadzu Corp., Tokyo, Japan). The sample was sandwiched between two pieces of BaF_2 slides and was melt-crystallized at different temperatures after melting at 190 °C for 2 min. Finally, it was cooled to ~23 °C for FTIR measurements. The spectra were accumulated with 64 scans and a resolution of 2 cm^{-1}.

Tensile Test. Tensile properties were measured on a Shimadzu (Tokyo, Japan) EZ test machine at a crosshead speed of 2 mm/min. All of the specimens have a gauge length of 22.25 mm, a gauge width of 4.76 mm, and a thickness of 0.35−0.40 mm. Seven specimens were tested for each material.

Dynamic Mechanical Thermal Analysis (DMTA). DMTA was performed on a DMS210 (Seiko Instruments, Tokyo, Japan) equipped with a SSC5300 controller at a frequency of 5 Hz and a heating rate of 2 °C/min. The samples were thin rectangular strips with dimensions of about 30 × 10 × 0.4 mm^3.

RESULTS AND DISCUSSION

Preliminary Structure of PPZn and Composites. In Figure 1 are compared the WAXD patterns of PPZn and quenched PLLA/PPZn composite samples. The WAXD pattern of PPZn displays an interlayer d spacing of 1.414 nm [estimated from the (010) reflection], together with multiple orders of this reflection. The interlayer distance of pure PPZn is in good agreement with that reported by Clearfield et al. (1.434 nm) (50). This indicates that the phenyl rings protrude into the interlamellar region beyond that of the phosphate group on both sides of the layer with enough phenyl−phenyl abutments to hold the layers apart. In the WAXD profiles of composites, the diffraction peak of PPZn is present without a discernible shift, and the intensity of the (010) reflection increases with the PPZn content. These results indicate that the PPZn layers were almost not exfoliated or intercalated by PLLA chains in the melt-mixing process, which may be due to the small interlayer spacing and/or strong interlayer force of PPZn. Chemical modification of the interlayer structure of PPZn is necessary to obtain the nanoscaled dispersion in the polymeric matrix, which will be focused in the future study.

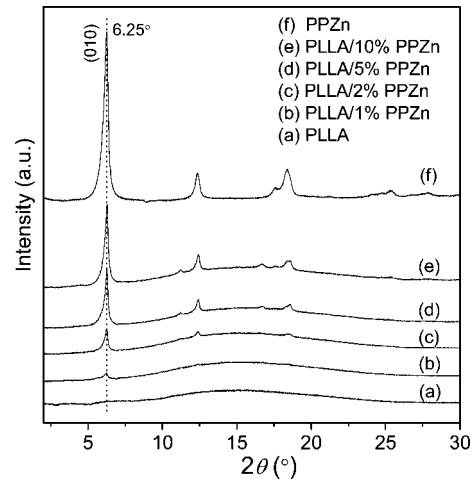

FIGURE 1. WAXD patterns of pure PPZn and quenched PLLA/PPZn composites with different PPZn loadings.

Nonisothermal Crystallization. The crystallization behavior of PPZn-containing PLLA was first compared with that of the PDLA- and talc-containing PLLAs. Talc is one of the most widely used NAs for semicrystalline polymers. Figure 2 shows the DSC curves of nonisothermal melt crystallization and subsequent heating scans for the neat PLLA and PLLAs containing 1% PPZn, PDLA, or talc. The crystallization of neat PLLA is very slow. Upon cooling at 10 °C/min, the crystallization peak is not detected and an exothermic cold-crystallization peak (near 115 °C) is observed in the following heating process. With the addition of 1% PDLA, a broad crystallization peak at ~97 °C appears in the DSC cooling curve. Although the crystallization of PLLA is enhanced by the incorporation of PDLA, a PLLA/1% PDLA sample cannot complete the crystallization upon cooling at 10 °C/min, as seen in Figure 2. Obviously, talc can accelerate the crystallization of PLLA, which completes upon cooling at 10 °C/min with the incorporation of 1% talc. This is coincident with the results of Li and Huneault (51). For PLLA containing 1% PPZn, the crystallization peak observed in the cooling process becomes much sharper and shifts to higher temperature by ~20 °C compared to PLLA containing the

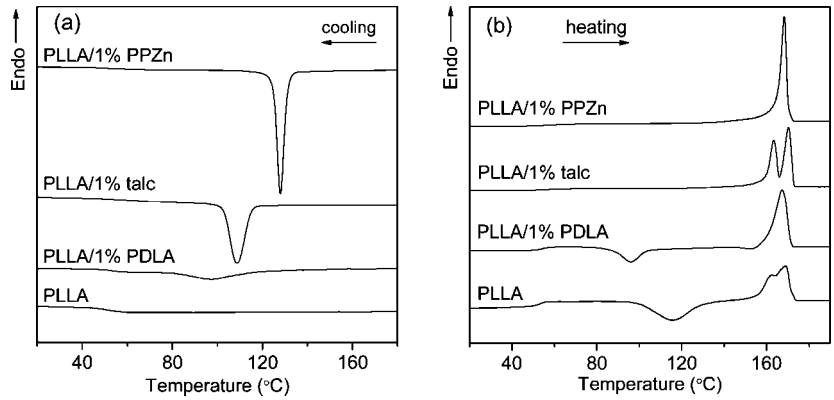

FIGURE 2. DSC curves of (a) nonisothermal melt crystallization and (b) subsequent melting for pure PLLA and PDLA-, talc-, and PPZn-containing PLLAs. Both the heating and cooling rates are 10 °C/min.

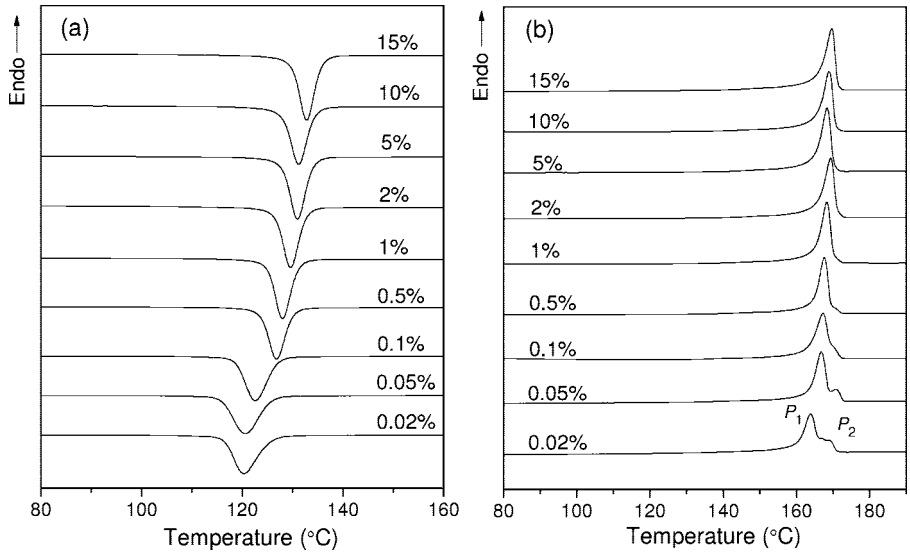

FIGURE 3. DSC curves of (a) nonisothermal melt crystallization and (b) subsequent melting for PLLA/PPZn samples with different PPZn contents. Both the heating and cooling rates are 10 °C/min.

same amount of talc. It can be concluded that PPZn accelerates the crystallization of PLLA significantly, and its effect on PLLA crystallization is much greater than that of talc and PDLA.

The effects of the PPZn content on the nonisothermal melt crystallization of PLLA were investigated by DSC. Figure 3 presents the DSC curves recorded during the cooling and subsequent heating processes for PLLA/PPZn samples with different PPZn contents. The thermal properties such as the melt-crystallization temperature (T_c) and degree of crystallinity (X_c) obtained from DSC analysis are plotted as a function of the PPZn content in Figure 4. X_c was estimated by comparing the melting enthalpy (ΔH_m) with the value of an infinitely large crystal (ΔH_m^0), taken as $\Delta H_m^0 = 93$ J/g (52) ($X_c = \Delta H_m/\Delta H_m^0 \times 100\%$).

The crystallization and melting behavior of PLLA depends on the PPZn content. As seen in Figure 3a, with the addition of 0.02% PPZn, the crystallization of PLLA is completed upon cooling, and the T_c value (~120 °C) is ~12 °C higher than that of PLLA containing 1% talc. With increasing PPZn content, the crystallization peak becomes sharp and shifts to higher temperature successively, which can be distinctly seen from Figure 4. On the other hand, as shown in Figures 3b and 4, X_c and the melting temperature (T_m) of PLLA increase progressively with increasing PPZn content. This is due to the effect of the crystallization temperature. With an increase of the PPZn loading, the crystallization of PLLA becomes faster, and the T_c value increases (Figure 3a).

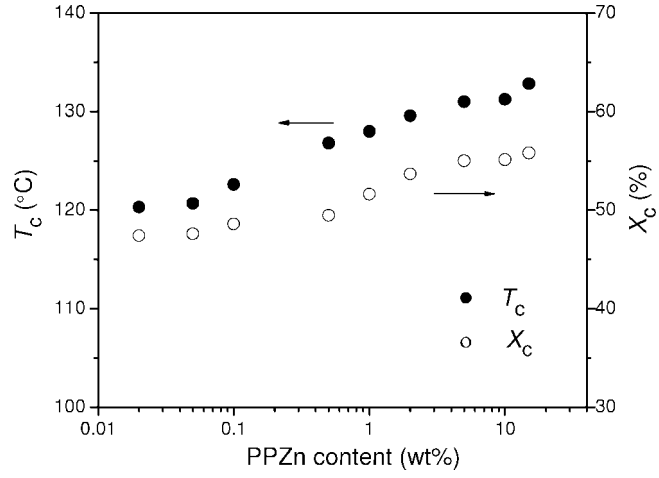

FIGURE 4. Dependence of the melt-crystallization temperature (T_c) and degree of crystallinity (X_c) of PLLA/PPZn samples on PPZn contents.

Generally, the crystals formed at higher T_c have larger laminar thickness and thus possess higher X_c and T_m.

As seen in Figure 3b, when the PPZn loading is more than 0.5%, only an endotherm appears in the DSC melting curve. However, with the incorporation of less than 0.5% PPZn, two melting peaks (or a melting peak and a peak shoulder at the high-temperature side) are observed. Previous studies (41−43) have reported that the melting behavior of PLLA depends on the crystallization temperature and crystalline structure. As will be described later, PPZn almost does not affect the crystalline structure of PLLA. So, it is considered that the difference between the melting behavior of the samples with various PPZn contents is caused by the effect of T_c. For all of these samples, the crystallization peak is in the high-temperature region (≥110 °C; Figure 3a), indicating that PLLA α crystals are mainly formed in this cooling process (41−43). When the PPZn loading is less than 0.5%, T_c is relatively lower and thus the less perfect crystals are formed. The samples undergo a melt recrystallization−remelting process upon heating. The lower temperature peak (P_1) is ascribed to the melting of primary crystals, and the higher temperature peak or shoulder (P_2) corresponds to the melting of the recrystallized crystals (41−43). With the addition of more than 0.5% PPZn, the T_c value is higher and thus perfect crystals are formed. The samples melt directly without the melt-recrystallization process, leading to the appearance of a single endothermic peak. As shown in Figure 2, the different melting behavior of PLLA/NA systems is also attributed to the effect of the crystallization temperature. Because of the relatively lower melt- or cold-crystallization temperature (105−120 °C), the neat PLLA and PLLA/1% talc sample undergo a melt-recrystallization process upon heating, with the appearance of two endothermic peaks.

Figure 5 shows the DSC traces of the quenched PLLA and composite samples collected upon heating at 10 °C/min. In addition to the glass transition, all of the DSC curves show an exothermic cold-crystallization peak and a melting peak at higher temperature. The values of the glass transition temperature (T_g), cold-crystallization temperature (T_{cc}), T_m, ΔH_m, and X_c are summarized in Table 1. As can be seen, no distinct change in T_g is observed upon the addition of PPZn. In the case of neat PLLA, a very broad crystallization peak at 124 °C and a small melting peak (ΔH_m = 20 J/g) are observed. The T_{cc} value of pure PLLA is clearly higher than that of PPZn-containing PLLA, and the ΔH_m value of pure PLLA is less than half of that of PPZn-containing PLLA. These results indicate that the cold crystallization of pure PLLA is much slower than that of PPZn-containing PLLA and pure PLLA cannot crystallize sufficiently in this heating process. With the addition of PPZn, the T_{cc} value decreases, indicating an enhancement in the crystallization rate. For the PPZn-containing PLLA, the X_c value is almost constant with an increase of the PPZn concentration.

When the DSC results shown in Figures 3b and 5 are compared, it is obvious that the melting behavior of PPZn-containing PLLA after melt and cold crystallization is different. This is attributed to the effect of the crystallization temperature. As seen in Figure 5, the crystallization temperature of PPZn-containing PLLA in the cold crystallization is in the low-temperature range (<110 °C), where the disordered α′ form is mainly developed (41−43). The α′-to-α crystalline phase transition takes place upon heating, resulting in an exotherm (P_{ex}) before the final melting peak (P_1) (41−43). Additionally, with a decrease in the PPZn content, the T_{cc} value increases, and the α′-form content in the cold-crystallized sample decreases. Thus, the exotherm P_{ex} decreases in magnitude. As seen in Figure 2, because of the low melt- and cold-crystallization temperatures, PLLA/1% PDLA sample also undergoes a phase transition process upon heating.

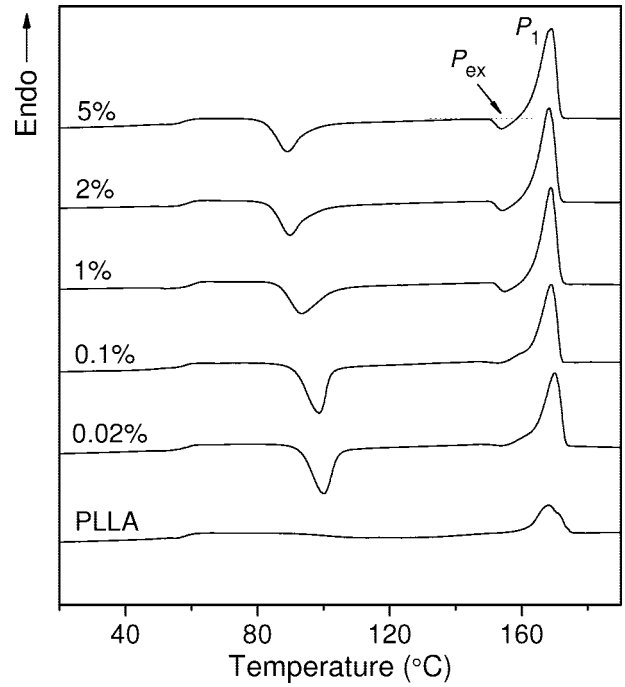

FIGURE 5. DSC curves of nonisothermal cold crystallization during heating at 10 °C/min for quenched PLLA and PLLA/PPZn samples with different PPZn contents.

Table 1. Nonisothermal Cold Crystallization of Quenched PLLA and Its Composites at a Heating Rate of 10 °C/min

sample	T_g (°C)	T_{cc} (°C)	T_m (°C)	ΔH_m (J/gPLLA)	X_c (%)
PLLA	58	124	168	20	22
PLLA/0.02% PPZn	57	100	168	42	45
PLLA/0.1% PPZn	59	99	167	42	45
PLLA/1% PPZn	59	93	169	42	45
PLLA/2% PPZn	59	90	168	42	45
PLLA/5% PPZn	58	89	169	43	46

Isothermal Crystallization. Because the crystallization rates of the PPZn-containing PLLA samples are very fast, in the DSC measurements they can crystallize upon rapid cooling (e.g., 100 °C/min) before the sample temperature reaches the desired T_c. Therefore, only the isothermal crystallization at a higher T_c region, i.e., 130−150 °C, was investigated. Figure 6 shows the DSC curves for neat PLLA and its composites crystallized at 130 and 140 °C. As can

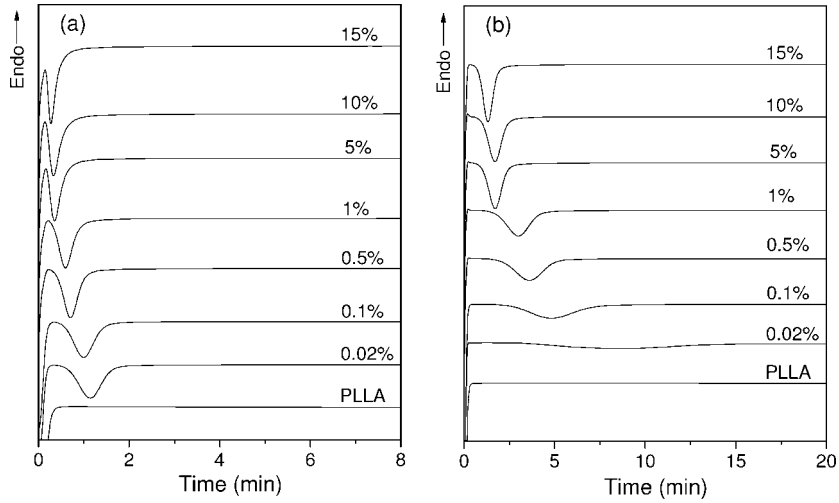

FIGURE 6. DSC curves of isothermal melt crystallization at (a) 130 and (b) 140 °C for PLLA/PPZn samples with different PPZn contents.

Table 2. Kinetic Parameters of Neat and PPZn-, Talc-, and PDLA-Containing PLLAs Isothermally Melt-Crystallizing at 130 and 140 °C

	T_c = 130 °C				T_c = 140 °C			
sample	$t_{1/2}$ (min)	n	k (min^{-n})	N(mm^{-3})	$t_{1/2}$ (min)	n	k (min^{-n})	N(mm^{-3})
PLLA	28.0	2.7	1.4×10^{-4}	8.2×10^{2}	60.2	2.9	5.4×10^{-6}	1.1×10^{2}
PLLA/0.02% PPZn	1.2	3.1	0.95	5.6×10^{6}	8.8	2.7	0.0043	8.5×10^{4}
PLLA/0.1% PPZn	1.0	3.1	2.1	1.3×10^{7}	4.9	3.0	0.022	4.3×10^{5}
PLLA/1% PPZn	0.63	2.8	7.9	4.6×10^{7}	3.0	3.1	0.064	1.3×10^{6}
PLLA/5% PPZn	0.41	2.1	13.1	7.7×10^{7}	1.8	3.2	0.21	4.1×10^{6}
PLLA/15% PPZn	0.33	2.1	16.3	9.6×10^{7}	1.4	3.0	0.28	5.5×10^{6}
PLLA/1% talc	6.79	2.6	8.8×10^{-3}	5.2×10^{4}	26.8	2.2	7.2×10^{-4}	1.4×10^{4}
PLLA/1% PDLA	6.37	2.7	4.0×10^{-3}	2.4×10^{4}	21.6	2.5	5.1×10^{-4}	1.0×10^{4}

be seen, the crystallization peak of neat PLLA is very broad. With the incorporation of PPZn and an increase in the PPZn content, the crystallization peak sharpens and the crystallization time shortens.

The Avrami equation is frequently employed to analyze the isothermal crystallization process of polymer, and its linear form can be stated as follows (53):

$$\log[-\ln(1 - X_t)] = \log k + n \log t \qquad (1)$$

where t is the crystallization time. X_t is the relative degree of crystallinity at a given time, which can be calculated from the integrated area of the DSC curve from $t = 0$ to t divided by the integrated area of the whole heat flow curve. n is the Avrami index, and k is the overall rate constant associated with both nucleation and growth contributions. The crystallization half-time $t_{1/2}$, defined as the time when X_t arrives at 50%, can be determined from the X_t vs t plot.

The kinetic parameters $t_{1/2}$, n, and k of neat and PPZn-, talc-, and PDLA-containing PLLAs are listed in Table 2. For PLLA/PPZn samples melt-crystallizing at T_c = 130, 140, and 150 °C, the $t_{1/2}$ values are plotted as a function of the PPZn concentration in Figure 7a. Because of the heterogeneous nucleation effect, $t_{1/2}$ reduces and k increases markedly with the addition of PPZn. In a previous paper (41), we have found that the neat PLLA shows a fastest melt crystallization at 100−110 °C; the $t_{1/2}$ value of neat PLLA crystallizing at T_c = 110 °C is ~32% of that of the sample crystallizing at 130 °C. PLLA is usually molded at this temperature range in practical processing (3). As shown in Table 2, the $t_{1/2}$ values of PLLA/1% and 15% PPZn samples crystallizing at 130 °C are less than 0.7 min. Upon crystallization at 100−110 °C, $t_{1/2}$ will be much shorter. So, it is considered that the crystallization of PPZn-containing PLLA is fast enough for industrial mold processing. On the other hand, with an increase in T_c, the degree of undercooling ($T_m^0 - T_c$) decreases, where T_m^0 denotes the equilibrium melting point. Thus, the crystallization rate decreases and the $t_{1/2}$ value increases with T_c, as seen in Figure 7a.

After isothermal crystallization, the melting behavior of PLLA/PPZn samples was examined by DSC. The samples crystallized at 130−150 °C show a single melting peak in the DSC curves (data not shown). The results of T_m and X_c are summarized in panels b and c of Figure 7, respectively. At the same T_c, the values of T_m and X_c are almost unaltered with an increase in the the PPZn content. With an increase of T_c, the more perfect crystals with larger lamellar thicknesses are generally formed, and thus both the values of T_m and X_c increase.

Spherulite Morphology. The spherulite morphology of PPZn-containing PLLA was compared with that of the neat and talc-containing PLLA samples by POM analysis. Figure 8 presents the POM photographs of neat PLLA, PLLA/1% talc, PLLA/0.02% PPZn, and PLLA/1% PPZn samples isothermally melt-crystallizing at 140 and 150 °C. As for neat PLLA, the spherulite size is very large and the spherulite

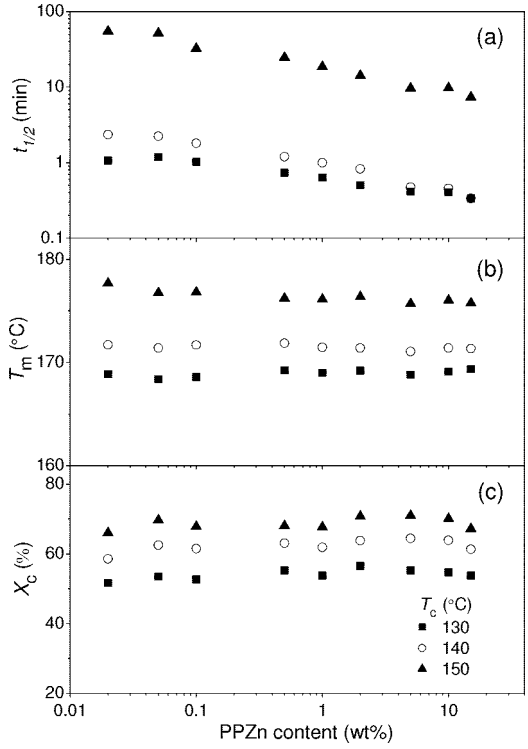

FIGURE 7. Dependence of (a) crystallization half-time ($t_{1/2}$), (b) melting temperature (T_m), and (c) degree of crystallinity (X_c) on the PPZn contents for PLLA/PPZn samples isothermally melt-crystallizing at 130, 140, and 150 °C.

density is small. With the addition of 1 % talc, the spherulite number increases slightly. With the incorporation of 0.02 % or 1 % PPZn, the spherulite size decreases dramatically, and the spherulite number is much larger than that of neat or talc-containing PLLA crystallized under the same conditions. This observation further confirms that PPZn has a more effective nucleation ability on the crystallization of PLLA than talc. With increasing PPZn concentration, the spherulite number further increases, which is consistent with the aforementioned DSC results. Besides, for a given sample, the spherulite number decreases with increasing T_c, because of the more difficult nucleation under the smaller degree of undercooling.

The effect of PPZn on the nucleation density was quantitatively analyzed. In the isothermal crystallization process, the nucleation density (N) can be estimated according to a model of three-dimensional spherulitic growth simultaneously initiated from active nuclei ($n \approx 3$) (12, 53):

$$N \approx 3k/4\pi G^3 \qquad (2)$$

where k is the Avrami rate constant, as shown in eq 1; G is the linear radius growth rate of spherulite, which can be determined from POM measurements. The G values of PLLA melt-crystallizing at 130 and 140 °C are 3.44 and 2.30 μm/min, respectively. A previous report (12) has indicated that NA almost does not change the spherulite growth rate of the polymers because NA only affects the primary nucleation but not the secondary nucleation. According to eq 2, the N values of neat and PPZn-, talc-, and PDLA-containing PLLAs were estimated, as shown in Table 2. With the incorporation of PPZn, the N value increases significantly, and it increases by 4−5 orders of magnitude with the addition of 1 % PPZn. Additionally, the N value further increases with an increase of the PPZn concentration. On the other hand, the PLLA/1 % PPZn sample exhibits a much smaller $t_{1/2}$ value and a larger N value than the talc- and PDLA-containing (1 %) PLLAs, indicating the larger nucleation effectiveness of PPZn.

Crystalline Structure. The effects of PPZn on the crystalline structure of PLLA were investigated by WAXD and FTIR measurements. Figure 9 shows the WAXD patterns of neat PLLA and PLLA/1 % PPZn samples melt-crystallized at low (80 °C) and high (140 °C) T_c's. For clarity, the enlarged patterns for the weaker peaks are shown in Figure 9b. Indexing of the observed reflections is based on the crystal structure reported for the PLLA α crystal by Miyata and Masuko (54). As seen in Figure 9, the WAXD patterns of the PLLA/1 % PPZn sample crystallized at high and low T_c are almost the same to those of the corresponding neat PLLA samples. For both the neat and PPZn-containing PLLA samples, with increasing T_c from 80 to 140 °C, the two strongest reflections, (110)/(200) and (203), shift to the higher 2θ side, and some weak reflections are present. Besides, only one reflection at nearby $2\theta = \sim 24.5°$ (indicated by the arrow) is observed for the neat and PPZn-containing PLLA samples crystallized at 80 °C, but two reflections, that is, (016) and (206) peaks of the α crystal, are present at this region as T_c was increased to 110 and 140 °C.

Figure 10 shows the T_c dependence of FTIR spectra in the carbonyl stretching region for the PLLA/1 % PPZn sample, which is very similar to that of neat PLLA. With increasing

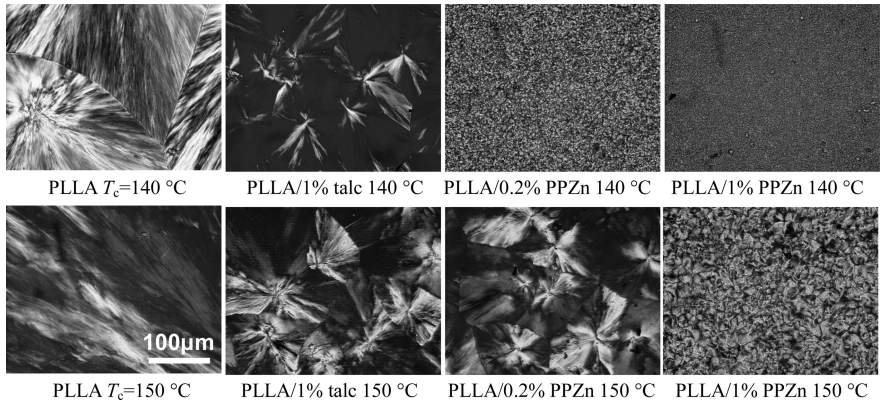

FIGURE 8. POM micrographs of pure PLLA and PLLAs containing 1% talc and 0.02% and 1% PPZn melt-crystallizing at 140 and 150 °C.

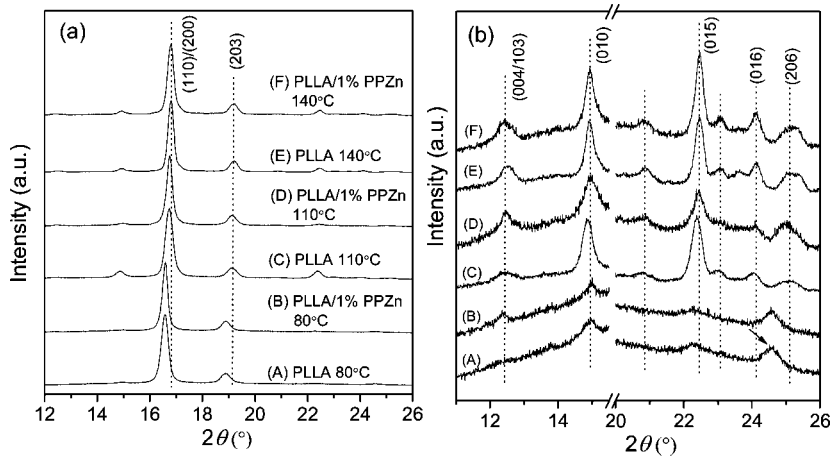

FIGURE 9. (a) WAXD profiles and (b) enlarged patterns of neat PLLA and PLLA/1% PPZn samples isothermally melt-crystallized at 80, 110, and 140 °C.

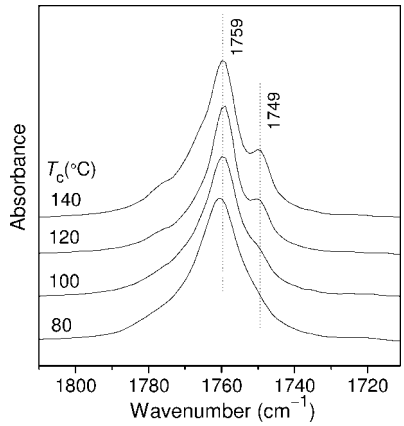

FIGURE 10. FTIR spectra in the carbonyl stretching region for the PLLA/1% PPZn sample isothermally melt-crystallized at 80−140 °C.

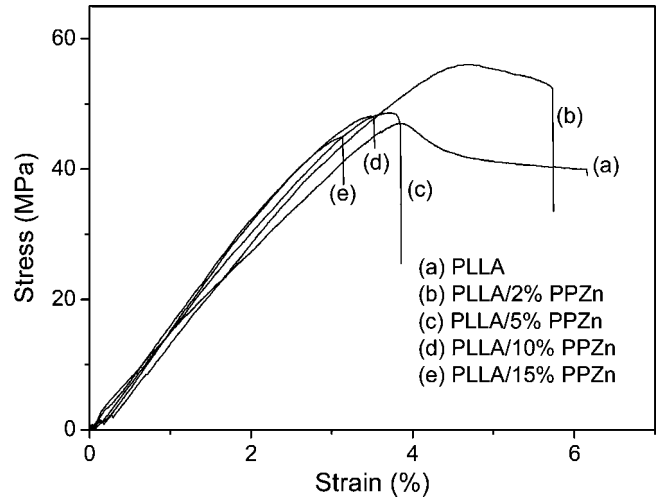

FIGURE 11. Representative stress−stain curves of neat PLLA and its composites.

Table 3. Static Mechanical Properties of PLLA and Its Composites

sample	tensile strength (MPa)	tensile modulus (GPa)	elongation at break (%)
PLLA	47 ± 2.5	1.43 ± 0.06	6.3 ± 0.52
PLLA/2% PPZn	56 ± 2.2	1.55 ± 0.08	5.9 ± 0.76
PLLA/5% PPZn	51 ± 2.3	1.65 ± 0.07	4.1 ± 0.81
PLLA/10% PPZn	46 ± 1.5	1.73 ± 0.09	3.9 ± 0.60
PLLA/15% PPZn	44 ± 2.5	1.84 ± 0.11	3.5 ± 0.29

T_c, the splitting band at 1749 cm^{-1}, which is characteristic of the α crystal, can be observed more and more clearly (41, 44). This is consistent with the WAXD data. From these results, it can be concluded that PPZn has no discernible effect on the crystalline structure of PLLA. Similar to neat PLLA, the α′ and α crystals of PLLA are predominantly formed in the PLLA/PPZn samples crystallized at low and high temperatures, respectively (41−44).

Proposed Nucleating Mechanism. Generally, the accelerated nucleation of the NA-containing polymers is caused by the mechanisms of chemical or epitaxial nucleation. Concerning the chemical nucleation, a chemical reaction between the polymer and NA occurs, resulting in the formation of a new nucleating compound which can induce the nucleation of other polymer chains. This mechanism has been used to explain the nucleation of PET/organic salt systems (55). According to the chemical structure, a chemical reaction is not expected to occur between PPZn and PLLA, and thus the chemical nucleation can be excluded.

As for epitaxial nucleation, the polymer crystals will epitaxially grow on the surface of NA. In this case, the growing of one crystal on the other is governed by the matching of the two lattice planes in contact (4, 56). This mechanism has been widely used to explain the nucleation of polymer/NA systems such as iPP/γ-quinacridone (5), iPP/4-fluorobenzoic acid (5), PET/talc (10), and so on. According to Cao et al. (49), the PPZn crystal possesses an orthorhombic cell with lattice parameters $a = 0.566$ nm, $b = 1.445$ nm, and $c = 0.480$ nm. In the PLLA α crystal, the chains pack in an orthorhombic or pseudoorthorhombic unit cell with dimensions $a = 1.034$ nm, $b = 0.597$ nm, and $c = 2.88$ nm (57). The length of the c axis of the PLLA α crystal is twice that of the b axis of the PPZn crystal, with a tiny mismatching of 0.3%. This excellent matching suggests that PLLA crystals might grow on the PPZn surface by an epitaxial mechanism, with the (001) lattice plane of PLLA along the (010) direction

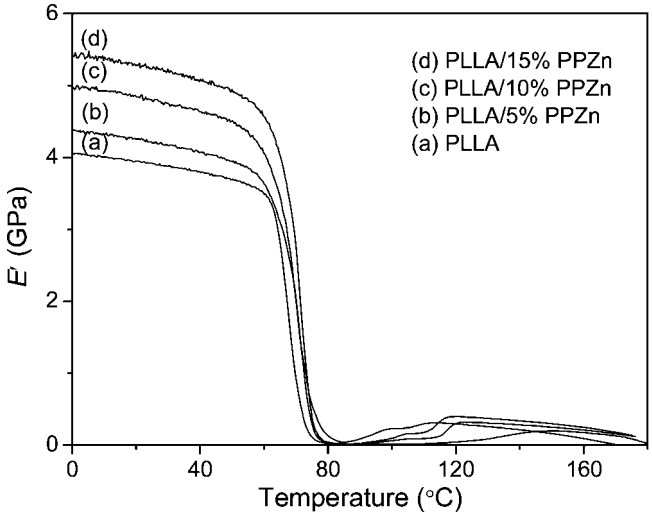

FIGURE 12. Temperature-dependent storage modulus (E') of neat PLLA and its composites.

of PPZn crystals. More in-depth experiments will be conducted to verify this proposal in a future study.

Tensile Test. The static mechanical properties of neat PLLA and its composites were investigated by the tensile test. Figure 11 shows the representative stress–strain curves of PLLA and its composites. The tensile strength, modulus, and elongation at break are summarized in Table 3. Neat PLLA shows a tensile strength of 47 MPa, a modulus of 1.43 GPa, and an elongation at break of 6.3%. As seen in Table 3, the tensile strength increases to 56 MPa, with the addition of 2% PPZn. This can be explained by the fact that the fillers are well wetted by the polymer matrix at lower content, which results in an efficient stress transfer from the matrix to the filler. Nevertheless, there is a decrease in the yield strength afterward when the PPZn content is larger than 5%. A possible explanation is due to the filler aggregation.

As seen in Table 3, the incorporation of PPZn improves the modulus of PLLA, signifying that stress transfers from the polymeric matrix to stiffer fillers occurred. The modulus of PLLA increases by 28% at 15% PPZn content. The elongation at break of the composite decreases with increasing PPZn content. When the PPZn loading is larger than 5%, the composites break before reaching the yield point in the tensile test. Generally, the addition of more fillers increases the probability of filler aggregation, which creates regions of stress concentrations that require less energy to elongate the crack propagation. During tensile deformation, the stress cannot transfer efficiently nearby these flaws, resulting in failure of the specimen. On the other hand, all of the elongation of the composite arises from the polymeric matrix because the filler is more rigid than the matrix. Hence, increasing the amount of filler decreases the amount of polymer available for elongation and thus decreases the elongation to break.

DMTA. The dynamic mechanical properties of composites were investigated by DMTA. Figure 12 shows the storage modulus (E') of neat PLLA and its composites as a function of the temperature. As can be seen, the storage modulus of PLLA/PPZn composites below T_g is higher than that of neat PLLA. The E' value (at 20 °C) of the composite containing 15% PPZn increases by ~34% compared to that of neat PLLA. Because of the glass transition, the E' value decreases greatly at ~60 °C. At temperatures higher than 80 °C, an increase in E' can be discerned for all of the samples, which is attributed to the cold crystallization. Because of the enhancement in the crystallization rate with the presence of PPZn, the increase in E' induced by the cold crystallization is more distinct and occurs at relatively lower temperature for the composites, as compared to neat PLLA. From these results, it can be concluded that the layered PPZn material is an effective filler to reinforce PLLA.

CONCLUSIONS

Layered metal phosphonate reinforced PLLA composites were fabricated, and their crystallization behavior and mechanical properties were investigated. The incorporation of PPZn significantly accelerates the crystallization of PLLA. With the addition of 0.02% PPZn, PLLA can finish the crystallization upon cooling at 10 °C/min, and the crystallization half-time decreases greatly. With increasing PPZn content, the rates of the cold and melt crystallizations of PLLA further increase. With the presence of PPZn, the nucleation density increases and the spherulite size reduces distinctly. The nucleation mechanism of the PLLA/PPZn system was proposed to be epitaxial nucleation. The incorporation of PPZn has no appreciable influence on the polymorphism of PLLA. Besides, PPZn shows good reinforcing effects on the PLLA matrix. Both the tensile and storage moduli of composites improve with increasing PPZn content. As a consequence, it is considered that layered metal phosphonate material is a new kind of benign filler for modifying the processability and mechanical properties of biodegradable PLLA materials, which might widen the applications of PLLA-related materials in the biomedical and conventional fields. Future studies will concentrate on the biodegradability as well as biocompatibility of these composites.

REFERENCES AND NOTES

(1) Gupta, B.; Revagade, N.; Hilborn, J. *Prog. Polym. Sci.* **2007**, *32*, 455.
(2) Im, S. S.; Kim, Y. H.; Yoon, J. S.; Chin, I. J. *Bio-Based Polymers: Recent Progress*; Wiley-VCH: Weinheim, Germany, 2005.
(3) Kawamoto, N.; Sakai, A.; Horikoshi, T.; Urushihara, T.; Tobia, E. *J. Appl. Polym. Sci.* **2007**, *103*, 198.
(4) Libster, D.; Aserin, A.; Garti, N. *Polym. Adv. Technol.* **2007**, *18*, 685.
(5) Mathieu, C.; Thierry, A.; Wittmann, J. C.; Lotz, B. *J. Polym. Sci., Part B: Polym. Phys.* **2002**, *40*, 2504.
(6) Blomenhofer, M.; Ganzleben, S.; Hanft, D.; Schmidt, H. W.; Kristiansen, M.; Smith, P.; Stoll, K.; Mäder, D.; Hoffmann, K. *Macromolecules* **2005**, *38*, 3688.
(7) Alcazar, D.; Ruan, J.; Thierry, A.; Lotz, B. *Macromolecules* **2006**, *39*, 2832.
(8) Mohmeyer, N.; Schmidt, H. W.; Kristiansen, P. M.; Altstädt, V. *Macromolecules* **2006**, *39*, 5760.
(9) Su, Z.; Dong, M.; Guo, Z.; Yu, J. *Macromolecules* **2007**, *40*, 4217.
(10) Haubruge, H. G.; Daussin, R.; Jonas, A. M.; Legras, R.; Wittmann, J. C.; Lotz, B. *Macromolecules* **2003**, *36*, 4452.
(11) Miyazaki, T.; Takeda, Y.; Akasaka, M.; Sakai, M.; Hoshiko, A. *Macromolecules* **2008**, *38*, 2749.
(12) He, Y.; Inoue, Y. *Biomacromolecules* **2003**, *4*, 1865.
(13) Alata, H.; Hexig, B.; Inoue, Y. *J. Polym. Sci., Part B: Polym. Phys.* **2006**, *44*, 1813.

(14) Qian, J.; Zhu, L.; Zhang, J.; Whitehouse, B. S. *J. Polym. Sci., Part B: Polym. Phys.* **2007**, *45*, 1564.
(15) Kai, W.; Zhu, B.; He, Y.; Inoue, Y. *J. Polym. Sci., Part B: Polym. Phys.* **2005**, *43*, 2340.
(16) Dong, T.; Kai, W.; Pan, P.; Cao, A.; Inoue, Y. *Macromolecules* **2007**, *40*, 7244.
(17) Schmidt, S. C.; Hillmyer, M. A. *J. Polym. Sci., Part B: Polym. Phys.* **2001**, *39*, 300.
(18) Anderson, K. S.; Hillmyer, M. A. *Polymer* **2006**, *47*, 2030.
(19) Tsuji, H.; Takai, H.; Saha, S. K. *Polymer* **2006**, *47*, 3826.
(20) Nam, J. Y.; Okamoto, M.; Okamoto, H.; Nakano, M.; Usuki, A.; Matsuda, M. *Polymer* **2006**, *47*, 1340.
(21) Mitomo, H.; Ohba, M.; Kasai, Y.; Ozawa, M. *Polym. Prepr. Jpn.* **2007**, *56*, 2277.
(22) Krikorian, V.; Pochan, D. J. *Chem. Mater.* **2003**, *15*, 4317.
(23) Ray, S. S.; Okamoto, M. *Macromol. Rapid Commun.* **2003**, *24*, 815.
(24) Chen, G.-X.; Kim, H.-S.; Shim, J.-H.; Yoon, J.-S. *Macromolecules* **2005**, *38*, 3738.
(25) Chen, G.-X.; Choi, J.-B.; Yoon, J.-S. *Macromol. Rapid Commun.* **2005**, *26*, 183.
(26) Chen, G.-X.; Yoon, J.-S. *Macromol. Rapid Commun.* **2005**, *26*, 899.
(27) Ray, S. S.; Yamada, K.; Okamoto, M.; Ueda, K. *Macromol. Mater. Eng.* **2003**, *288*, 203.
(28) Qiu, X.; Hong, Z.; Hu, J.; Chen, L.; Chen, X.; Jing, X. *Biomacromolecules* **2005**, *6*, 1193.
(29) Sun, L.; Boo, W. J.; Sun, D.; Clearfield, A.; Sue, H. J. *Chem. Mater.* **2007**, *19*, 1749.
(30) Boo, W. J.; Sun, L. Y.; Liu, J.; Clearfield, A.; Sue, H. J.; Mullins, M. J.; Pham, H. *Compos. Sci. Technol.* **2007**, *67*, 262.
(31) Zhang, R.; Hu, Y.; Li, B.; Chen, Z.; Fan, W. *J. Mater. Sci.* **2007**, *42*, 5641.
(32) Brandao, L. S.; Mendes, L. C.; Medeiros, M. E.; Sirelli, L.; Dias, M. L. *J. Appl. Polym. Sci.* **2006**, *102*, 3868.
(33) Alberti, G.; Costantino, Y.; Marmottini, F.; Vivani, R.; Zappelli, P. *Angew. Chem., Int. Ed. Engl.* **1993**, *32*, 1357.
(34) Zhang, B.; Clearfield, A. *J. Am. Chem. Soc.* **1997**, *119*, 2751.
(35) Wright, P. A.; Jones, R. H.; Natarajan, S.; Bell, R. G.; Chen, J.; Hursthouse, M. B.; Thomas, J. M. *J. Chem. Soc., Chem. Commun.* **1993**, *633*.
(36) Bellitto, C.; Federici, F.; Ibrahim, S. A. *J. Chem. Soc., Chem. Commun.* **1996**, *759*.
(37) Jaber, M.; Larlus, O.; Miehe-Brendlé, J. *Solid State Sci.* **2007**, *9*, 144.
(38) Dorozhkin, S. V.; Epple, M. *Angew. Chem., Int. Ed.* **2002**, *41*, 3130.
(39) Bujoli, B.; Lane, S. M.; Nonglaton, G.; Pipelier, M.; Léger, J.; Talham, D. R.; Tellier, C. *Chem.—Eur. J.* **2005**, *11*, 1980.
(40) Herschke, L.; Lieberwirth, I.; Wegner, G. *J. Mater. Sci.: Mater. Med.* **2006**, *17*, 95.
(41) Pan, P.; Kai, W.; Zhu, B.; Dong, T.; Inoue, Y. *Macromolecules* **2007**, *40*, 6898.
(42) Zhang, J.; Tashiro, K.; Tsuji, H.; Domb, A. J. *Macromolecules* **2008**, *41*, 1352.
(43) Yasuniwa, M.; Sakamo, K.; Ono, Y.; Kawahara, W. *Polymer* **2008**, *49*, 1943.
(44) Pan, P.; Zhu, B.; Kai, W.; Dong, T.; Inoue, Y. *Macromolecules* **2008**, *41*, 4296.
(45) Iwata, T.; Doi, Y. *Macromol. Chem. Phys.* **1999**, *200*, 2429.
(46) Furuhashi, Y.; Iwata, T.; Kimura, Y.; Doi, Y. *Macromol. Biosci.* **2003**, *3*, 462.
(47) Iwata, T.; Aoyagi, Y.; Tanaka, T.; Fujita, M.; Takeuchi, A.; Suzuki, Y.; Uesugi, K. *Macromolecules* **2006**, *39*, 5789.
(48) Zhu, B.; He, Y.; Nishida, H.; Yazawa, K.; Ishii, N.; Kasuya, K.; Inoue, Y. *Biomacromolecules* **2008**, *9*, 1221.
(49) Cao, G.; Lee, H.; Lynch, V. M.; Mallouk, T. E. *Inorg. Chem.* **1988**, *27*, 2781.
(50) Frink, K. J.; Wang, R. C.; Colón, J. L.; Clearfield, A. *Inorg. Chem.* **1991**, *30*, 1438.
(51) Li, H.; Huneault, M. A. *Polymer* **2007**, *48*, 6855.
(52) Fischer, E. W.; Sterzel, H. J.; Wegner, G. *Kolloid Z. Z. Polym.* **1973**, *251*, 980.
(53) Gedde, U. W. *Polymer Physics*; Chapman & Hall: London, 1995; pp 169—198.
(54) Miyata, T.; Masuko, T. *Polymer* **1997**, *38*, 4003.
(55) Legras, R.; Mercier, J. P.; Nield, E. *Nature* **1983**, *304*, 432.
(56) Okada, K.; Watanabe, K.; Urushihara, T.; Toda, A.; Hikosaka, M. *Polymer* **2007**, *48*, 401.
(57) Hoogsteen, W.; Postema, A. R.; Pennings, A. J.; Ten Brinke, G.; Zugenmaier, P. *Macromolecules* **1990**, *23*, 634.

AM800106F